Journal of Applied Polymer Science

Self-Structured Serrated Edges of Chemically Oxidized Poly(dimethylsiloxane) Disks

Masashi Watanabe, Kensuke Shinoda
Faculty of Textile Science and Technology, Shinshu University, 3-15-1 Tokida, Ueda, Nagano 386-8567, Japan
Correspondence to: M. Watanabe (E-mail: mwatana@shinshu-u.ac.jp)

ABSTRACT: Serrated structures on a micrometer scale were spontaneously formed along the edge of a poly(dimethylsiloxane) (PDMS) disk using the following procedure. First, a drop of PDMS prepolymer was placed on a glass slide, followed by vulcanization. Second, the obtained PDMS disk was soaked in a mixture of sulfuric acid and nitric acid to form a serrated structure. Consideration of the mechanism of the structure formation was based on the following results. (1) The acid oxidized the PDMS surface, which was then swollen with the acid mixture or water to form wrinkles. (2) The wrinkle wavelength depended on the thickness of the PDMS film. (3) The thickness of the PDMS disk varied near its edge because the meniscus of the drop of the PDMS prepolymer was retained after the vulcanization. These results suggest that the thickness gradient of the PDMS disk led to the spontaneous formation of a serrated edge structure. © 2014 Wiley Periodicals, Inc. J. Appl. Polym. Sci. **2014**, *131*, 40767.

KEYWORDS: elastomers; self-assembly; surface and interfaces; swelling

Received 7 January 2014; accepted 24 March 2014
DOI: 10.1002/app.40767

INTRODUCTION

Self-structuring on a nano- and micrometer scale is a recent topic in (bio)chemistry, physics, and materials science and technology. Although photolithography and electron-beam lithography are top-down approaches that are widely used for producing nano- and micro-objects or structures, they usually require expensive equipment and multiple time-consuming processes. Moreover, they are essentially limited to 2-dimensional patterns[1] and predicted to meet with the limitation of down sizing in the near future. To overcome such disadvantages and limitations, various bottom-up technologies using supramolecular self-assembly have been extensively explored for the past few decades.[2–4] Such technologies utilize noncovalent bonding between molecules (e.g., host-guest chemistry), interfaces, and micelles.

Supramolecular self-assemblies of a few molecules have been utilized for binding host and guest molecules and achieving molecular-sized machines.[2] However, it is still challenging to construct objects of a size visible to the naked eye using this technique because such supramolecules are objects on a nanometer scale. Association with other techniques that can produce larger objects on a micrometer or millimeter scale is needed. Although conventional photolithographic techniques are promising candidates for such association, we think that various self-structuring phenomena observed in nature should also be investigated.

Examples of self-assembly processes utilizing interfaces include layer-by-layer, Langmuir–Blodgett, and self-assembled monolayer methods; these have versatile applications in physics, (bio)chemistry, and medicine.[5,6] These methods can produce films whose thicknesses are on a nanometer scale, but whose areas can be square centimeters or greater. If the films prepared on surfaces whose topography is well defined, novel applications will be developed in the future. Thus, we think that the combination of technologies related to self-assembled films and surface topography will increase in importance.

Self-assembled micelle structures have been utilized as a bottom-up technology for preparing inorganic mesoporous materials.[7–9] Such structures are used as templates during the reaction of a precursor that is later converted into an inorganic material such as silica. Because the materials have well-defined pore structures, various applications, for example, sensors and drug delivery, have been proposed. Although forms of mesoporous materials are usually powder or film,[10] monodisperse microspheres are also possible.[11] If such microspheres are regularly arranged on a surface whose topography is well defined on a micrometer scale, hierarchical control of structures will be achieved. If the surface topography is also controlled using a self-structuring phenomenon, the structure will be completely

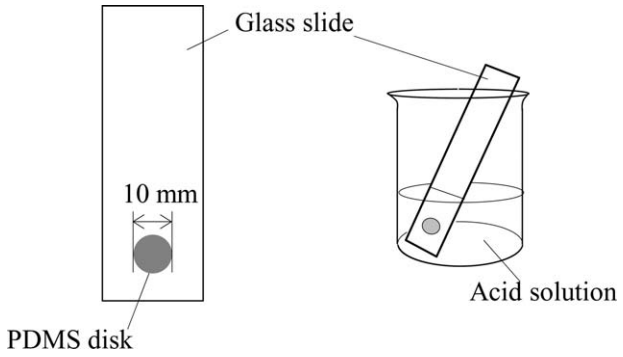

Figure 1. Experimental procedure. A PDMS disk was prepared on a glass slide and soaked in acid solution.

controlled by self-structuring phenomena ranging from nano- to centimeter scales.

Thus, we think that the combination of the control of surface topography with the self-assembly of molecules will be important in materials science and technology. In addition, although conventional photolithographic techniques can be used for controlling surface topographies, self-structuring phenomena should also be investigated for the same purpose.

In this study, we focus on buckling instability as such a self-structuring phenomenon where regular wrinkles form in a thin film on top of a thick elastic substrate. One such example, on a quite different scale, is the process of mountain formation by the folding of the earth's crust by buckling instability.[12] Wrinkles on a micrometer scale can also be created, for example, using a thin gold film on top of a thick poly(dimethylsiloxane) (PDMS) substrate.[13,14] Buckling instability is expected as a useful phenomenon for creating surface microstructures because well-ordered wrinkles are obtained when a homogeneous material, such as PDMS, is used as a substrate.[15–18]

The materials used as thin films can be evaporated or sputtered metals,[19,20] spin-coated polymers,[21] and silica-like materials formed by modifying the surface of a PDMS substrate using a UV-ozone treatment.[22,23] Such silica-like materials can be also obtained using chemical oxidation with a mixture of sulfuric acid and nitric acid.[24] Although this method does not require any expensive reagents and equipment, wrinkles with a well-ordered stripe pattern can be obtained.[25]

Patterns of wrinkling that have been reported so far are not only simple stripe, but also herringbone,[26,27] spoke,[28] target,[28]

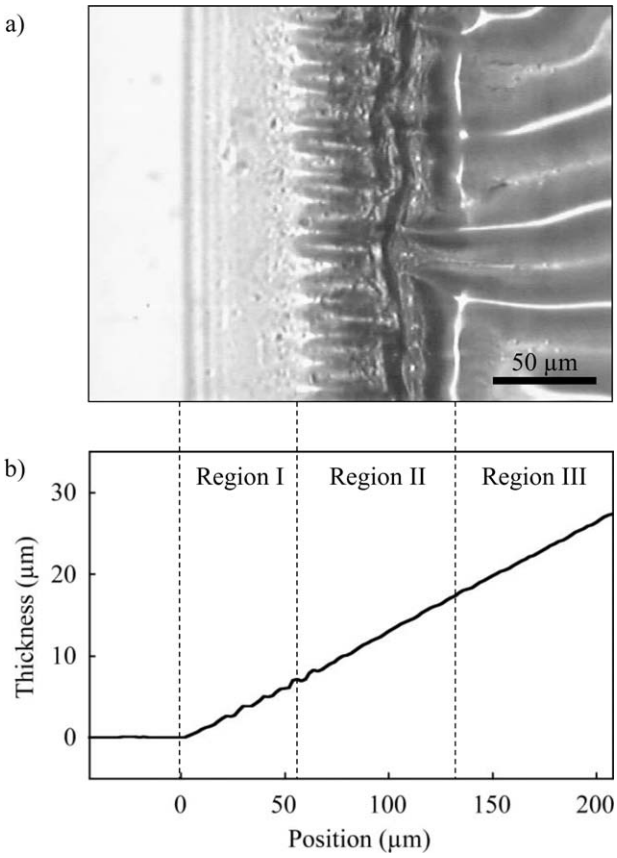

Figure 3. (a) Light microscope image near edge of PDMS disk oxidized by acid solution. (b) Thickness profile of disk measured before oxidation.

and checkerboard patterns.[23,29] Although these patterns were observed on the surfaces of samples, in this study, we focused on wrinkles near the edges of samples and found that serrated structures on a micrometer scale were formed by chemical oxidation of PDMS. Because serrated structures can be seen not only in natural objects, such as plant leaves,[30] but also in artificial objects, such as gear wheels, this method is potentially useful as an alternative technique for manufacturing micro- and nano-scale objects.

EXPERIMENTAL

Materials

PDMS prepolymers (KE-109-A and KE-109-B) were purchased from Shin-Etsu Chemical Co., Ltd. (Tokyo, Japan). Both

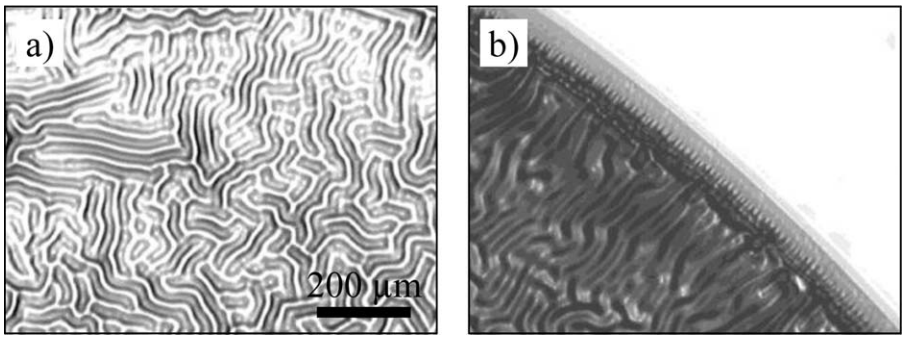

Figure 2. Light microscope images at the (a) center and (b) edge of PDMS disk.

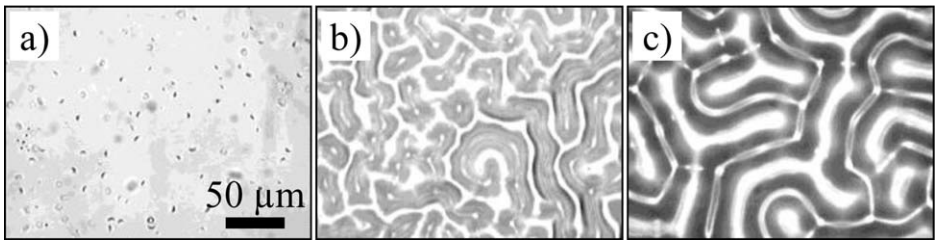

Figure 4. Light microscope images of the PDMS films spin-coated on a glass slide and then soaked in acid for 50 s at 80°C. The thicknesses were (a) 5.5, (b) 12, and (c) 35 μm.

prepolymers did not contain any solvent. Concentrated sulfuric acid (>95%) and concentrated nitric acid (60–61 wt %) were acquired from Wako Pure Chemical Industries, Ltd. (Osaka, Japan).

Preparation of PDMS Disk

PDMS prepolymers, KE-109-A and KE-109-B (50/50 wt %, the standard ratio that the manufacturer recommended), were mixed and degassed under vacuum. A drop (10 mg) of the mixture was placed on a glass slide (76 mm × 26 mm) that was pre-cleaned using a UV-ozone cleaner (UV-TC-110, Bioforce Nanosciences, Inc., Ames, IO). The glass slide was then stored at room temperature for 1 h until the diameter of the drop reached equilibrium. The drop was vulcanized in an oven at 100°C for 1 h. The obtained PDMS disk was 10 mm in diameter.

Measurement of Thickness Profile of PDMS Disk

The thickness profile was measured using a laser surface profiler (LT-9000, Keyence Corporation, Osaka, Japan).

Preparation of Acid Solution

An acid solution was prepared by mixing concentrated sulfuric acid, concentrated nitric acid, and distilled water (66/22/12 vol %). This solution (40 mL) was stirred in a beaker at 80°C for 50 min in order to decrease its excessive reactivity.[25]

Oxidation of PDMS Disk Surface

A PDMS disk prepared on a glass slide was soaked in the acid solution at 80°C for 30–70 s (Figure 1) immediately followed by washing with water at room temperature.

Preparation of PDMS Film

A mixture of the PDMS prepolymer was spin-coated on a glass slide using a spin-coater (1H-DX2, Mikasa Co., Ltd., Tokyo, Japan). The mixture was then vulcanized in an oven at 100°C for 1 h. The thickness of the obtained film was measured using a laser surface profiler (LT-9000, Keyence Corporation, Osaka, Japan).

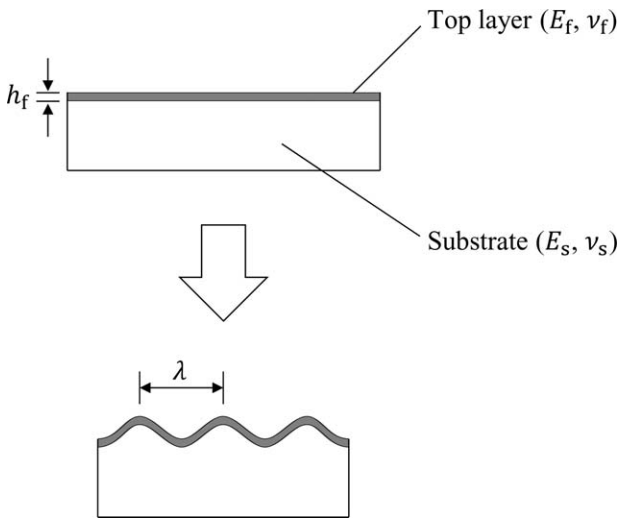

Figure 5. Wrinkling of film on top of thick, elastic substrate.

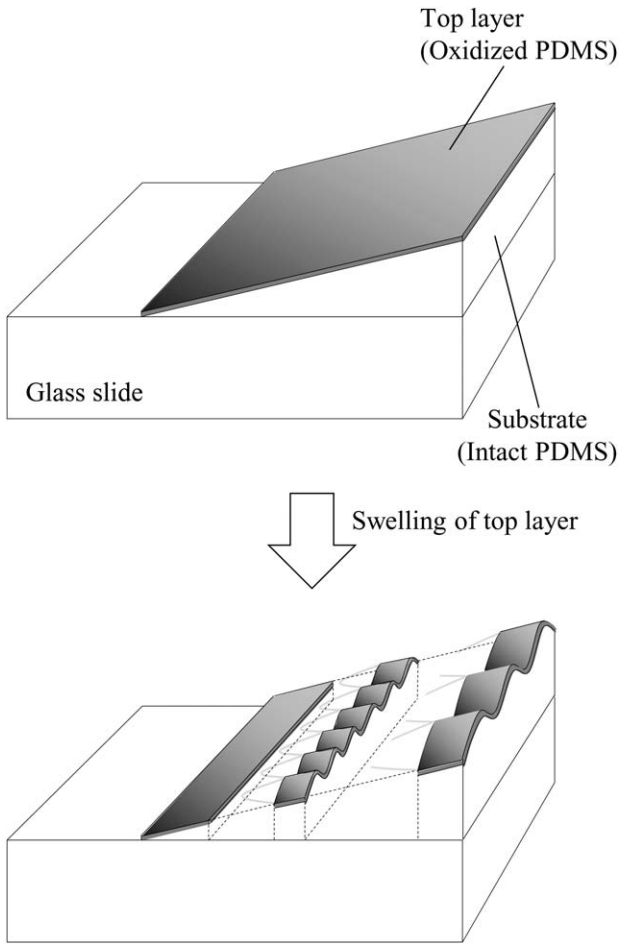

Figure 6. Schematic illustration of formation of serrated structure.

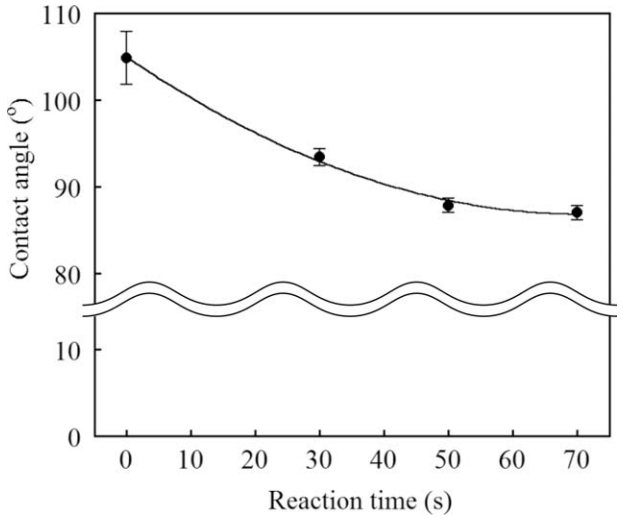

Figure 7. Contact angles of water on PDMS surfaces oxidized by acid solution at 80°C.

Measurement of Contact Angle

PDMS films (ca. 0.13 mm thick) prepared on a glass slide were treated with acid solution, washed with water, and finally dried at 60°C for 1 h. A water drop (3 μL) that was carefully placed on the surface was photographed to measure the contact angle.

RESULTS AND DISCUSSION

Formation of Serrated Structures

A PDMS disk on a glass slide was soaked in acid solution for 50 s at 80°C and then washed with water at room temperature. Using a light microscope, we observed wrinkles at the center of the disk surface [Figure 2(a)]. As previously reported,[25] the swelling of the surface that was oxidized by the acid solution was the cause of the wrinkling. We also found a serrated structure along the edge of the disk [Figure 2(b)], which is the focus of this article. (Before treatment with the acid solution, no serrated structure was observed.)

A light microscope image revealed that the disk edge could be divided into three regions (Regions I, II, and III) having distances in the ranges 0–55, 55–130, and >130 μm from the edge [Figure 3(a)]. In Region I, no wrinkles were observed. In Region II, there was a serrated structure in which small wrinkles similar to nails were regularly aligned at intervals of about 15 μm. In Region III, the wrinkles had a larger wavelength (ca. 45 μm). The thickness profile of the disk, which was measured before being soaked in the acid solution, showed thicknesses in the ranges 0–7, 7–17, >17 μm for each region [Figure 3(b)], suggesting that the thickness gradient might affect the wrinkling. The profile also showed that the contact angle of the mixture of PDMS prepolymers was 7.5°.

PDMS films with various thicknesses were prepared by spin-coating a mixture of prepolymers on glass slides. The films were soaked in acid solution and observed using a light microscope. As a result, no wrinkles were observed on 5.5-μm thick film [Figure 4(a)]. This result was consistent with the result that there were no wrinkles in Region I. It also suggested that wrinkling might be restricted by the glass slide beneath the PDMS film. On 12- and 35-μm thick films, the observed wrinkles had wavelengths of about 24 and 41 μm, respectively [Figure 4(b,c)]. Thus, the wrinkle wavelength increased with the increase in film thickness. This suggested that the difference in the thickness of the disk between Regions II and III [Figure 3(b)] might cause the difference in

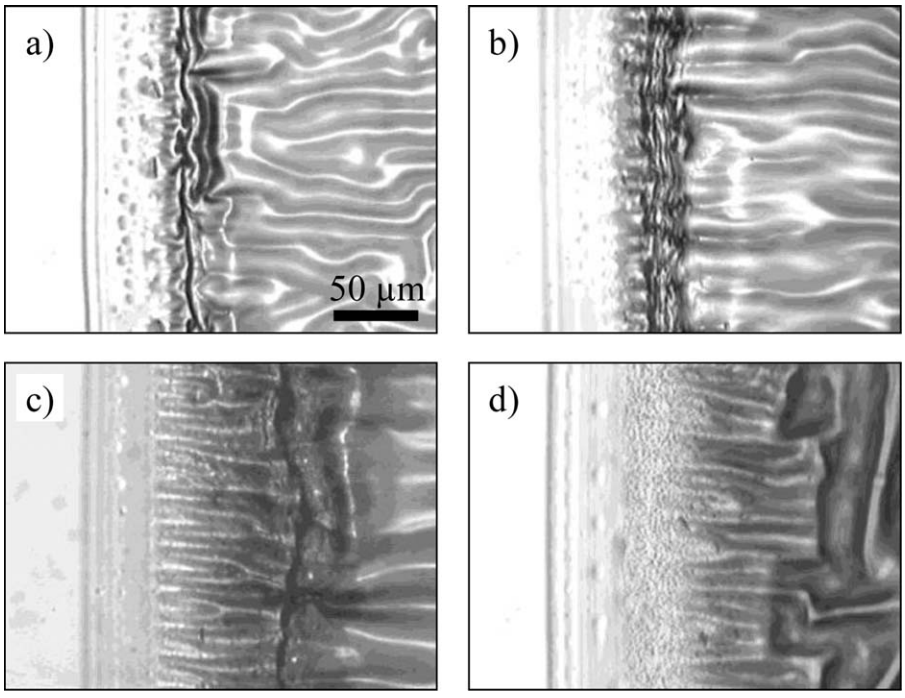

Figure 8. Edges of PDMS disks that were soaked in acid solution for (a) 30, (b) 40, (c) 60, (d) 70 s at 80°C.

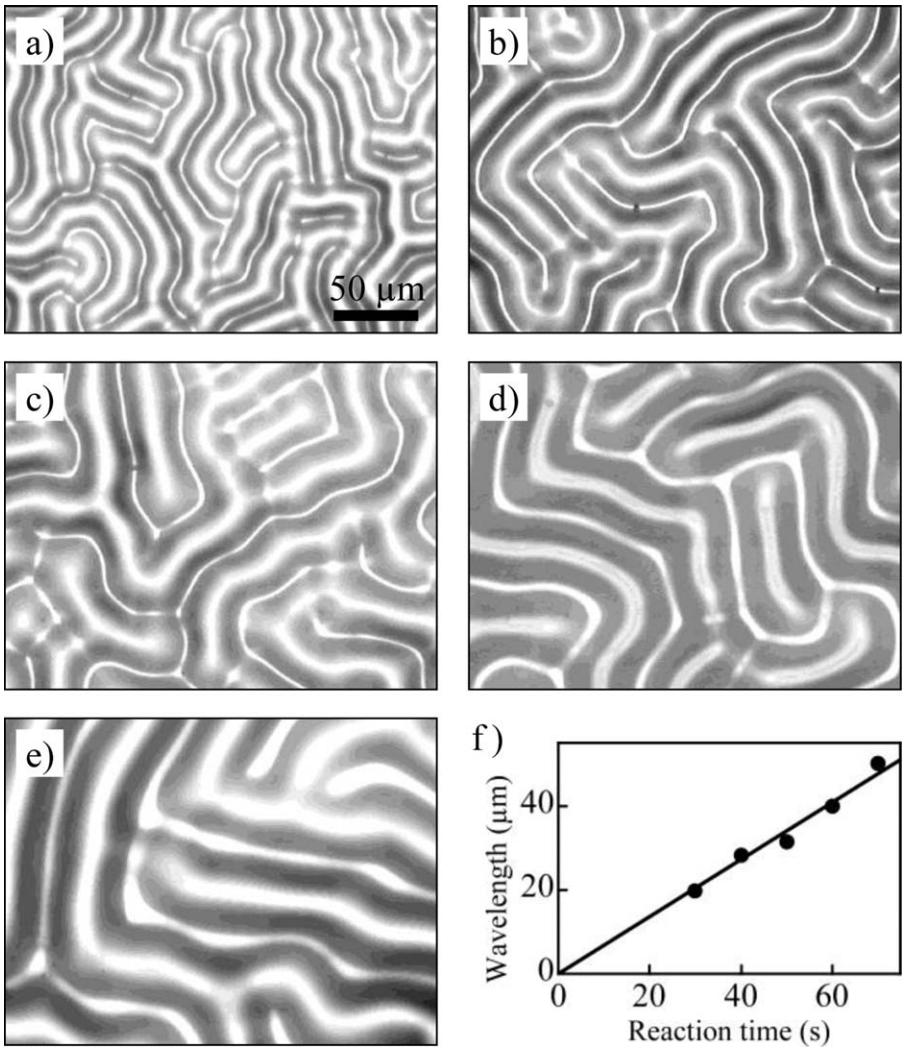

Figure 9. Wrinkles at the center of PDMS disks that were soaked in acid solution for (a) 30, (b) 40, (c) 50, (d) 60, and (e) 70 s at 80°C. (f) Relationship between reaction time and wrinkle wavelength.

wrinkle wavelength [Figure 3(a)]. As an additional experiment, we measured the wavelength of the wrinkles on a 195-μm thick film as about 44 μm. Thus, when the thickness was greater than 35 μm, the wavelength was almost independent of the thickness.

As previously reported, the acid solution oxidized the surface of the PDMS and formed a thin hydrophilic layer.[25] In general, such a thin layer on top of a thick elastic substrate can be wrinkled by in-plane compressive stress because of buckling instability.[31] In this study, the elastic substrate corresponded to the intact PDMS layer underlying the oxidized top layer and the in-plane compressive stress was induced by the swelling of the oxidized layer with water or the acid solution.

As is well known (see Figure 5), when the substrate (Young's modulus E_s and Poisson's ratio v_s) is much thicker than the top layer (Young's modulus E_f, Poisson's ratio v_f, and thickness h_f), the wrinkle wavelength, λ, is written as[31]

$$\lambda = 2\pi h_f \left\{ \frac{(1-v_s^2)E_f}{3(1-v_f^2)E_s} \right\}^{1/3} \quad (1)$$

However, in this study it could not be stated that the "substrate" (i.e., the intact PDMS layer) was much thicker than the top layer (i.e., the oxidized PDMS layer) because the substrate was 0–17 μm thick in Regions I and II and the top layer was assumed to be around 1 μm thick (see Ref. 25). In addition, the substrate was tightly bonded to the glass slide; it could not be peeled off, although it could be scraped off. Therefore, the substrate would function as a material that was stiffer than a thick and free substrate. Because the above equation means that a stiffer (i.e., greater E_s) substrate produces a smaller wavelength, it seems reasonable that the wrinkle wavelength decreased with the decrease in the thickness of the substrate, as shown in Figure 3(a,b). As the thickness gradually decreased, the wrinkle wavelength also decreased, resulting in the formation of an array of tapered structures (i.e., the serrated structure), as illustrated in Figure 6.

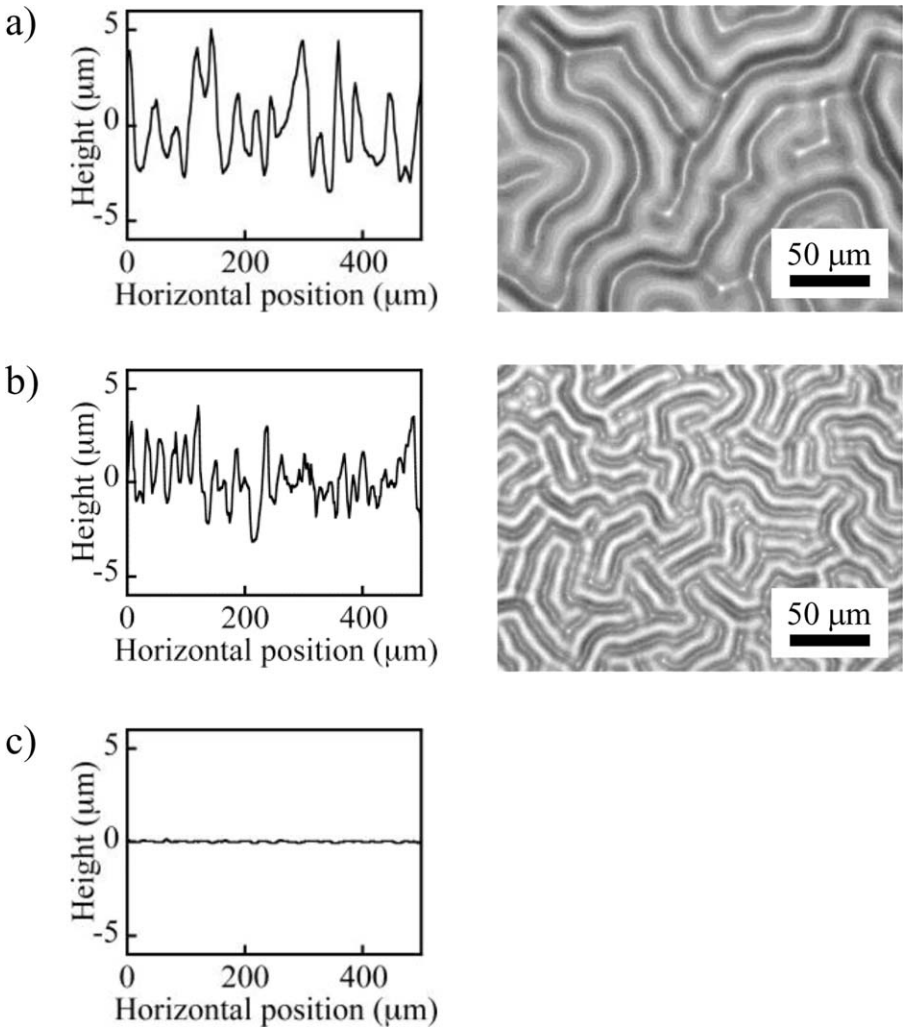

Figure 10. Profiles and light microscope images of wrinkles formed by soaking PDMS films in acid solution at (a) 80, (b) 60, and (c) 40°C for 50 s.

We also measured the contact angles of water on the PDMS surfaces oxidized by the acid solution. As reaction time increased, the contact angle decreased (Figure 7), indicating that the surface became hydrophilic. However, the decrease was moderate for the following reason. In general, a water drop still "senses" the underlying hydrophobic layer due to long-range interactions, even if the surface is covered with a thin hydrophilic layer.[32]

Control of Size of Serrated Structures

A PDMS disk was soaked in the acid solution at 80°C using various reaction times (30–70 s). The length and width of the

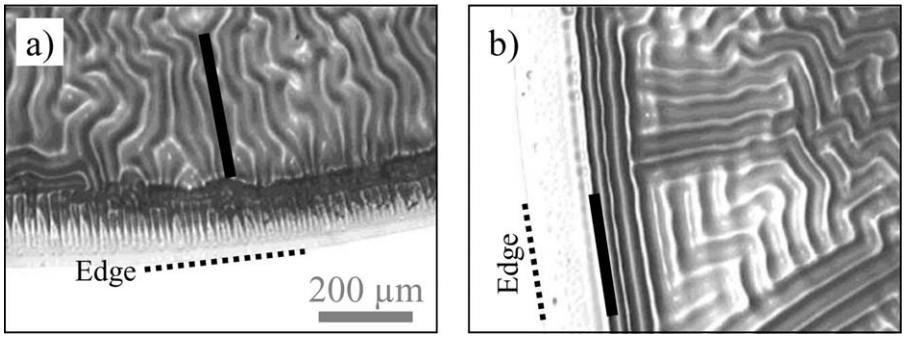

Figure 11. Light microscope images near edge of PDMS disk that (a) had nail-like structures and (b) did not have them. The sample was soaked in acid solution for 60 s at 80°C.

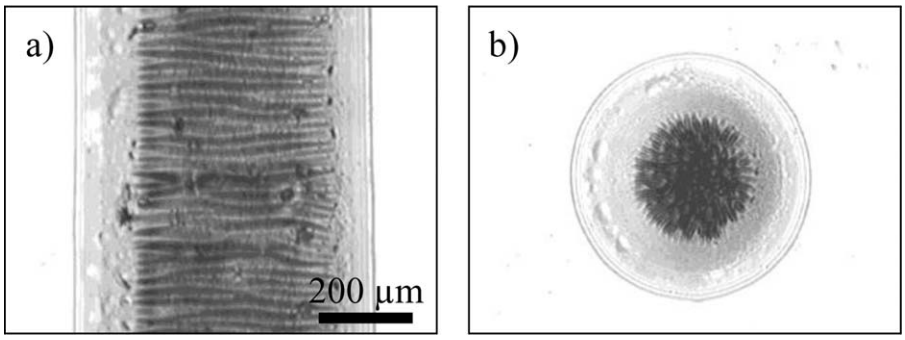

Figure 12. Samples (a) 630 μm wide and (b) 510 μm in diameter. The samples were soaked in acid solution for 60 s at 80°C.

small wrinkles resembling nails along the edge increased with an increase in reaction time, as shown in Figures 8(a–d) and 3(a). The wrinkle wavelength at the center of the disk also increased [Figure 9(a–f)], suggesting that a longer reaction time formed a thicker and/or stiffer top layer on the basis of eq. (1).

The dependency of the wrinkling on the reaction temperature was also examined. PDMS films (ca. 0.13 mm thick) were soaked in the acid solution for 50 s at 80, 60, and 40°C. Although wrinkles were formed in the films treated at 80 and 60°C, no wrinkles were observed in the film treated at 40°C (Figure 10). Therefore, in most of the experiments in this study, we selected 80°C as the reaction temperature.

Serrated Structures Obtained Using Small Samples

When the PDMS sample was a disk with a diameter 10 mm, there were nail-like structures along the edge [Figure 11(a)], but there were also portions where the edge did not have such structures [Figure 11(b)]. However, the following characteristic relationship was found. When the wrinkles that formed about 150 μm apart from the edge [marked with a thick line in Figure 11(a)] were perpendicular to the edge (marked with a dotted line), the nail-like structures were observed. However, when the wrinkles were parallel to the edge [Figure 11(b)], no such structures were observed. Although we have not yet fully clarified what factor determined the direction of the wrinkles, the direction seemed to be related to which part of the sample was first in contact with the surface of the acid solution (or the water) during the oxidation (or washing) process. To selectively create wrinkles with such two directions is still an issue that should be resolved through further studies.

However, such an issue did not exist when we used small samples whose width was less than several hundred micrometers because the wrinkles formed more than 150 μm apart from the edge. For example, when the sample width was 630 μm, only the nail-like structures were formed [Figure 12(a)]. When the sample was a tiny disk with a diameter of 510 μm, a starburst shape was obtained [Figure 12(b)]. Thus, various objects that had a serrated structure could easily be created by only soaking PDMS samples in the acid solution.

In recent studies by other groups, the wrinkling pattern of a small circular area in a large elastic sheet were theoretically and experimentally investigated and patterns similar to Figure 12(b) were observed.[33,34] In contrast, because we utilized the edges of elastic sheets in order to control the wrinkling pattern, the control mechanism was different from that of those studies.

Finally, we provide further explanation of the two different causes of wrinkling: swelling and mechanical compression. In this study, PDMS samples were soaked in acid solutions at 80°C, immediately followed by washing with water at room temperature. The wrinkles that were obtained were formed by the swelling of the sample surface that was oxidized by the acid solution. In contrast, in our earlier study,[25] the samples oxidized by the acid solution were washed after being cooled at room temperature in air, and very slight wrinkles were observed. However, because the surface was hardened by the oxidation, we were able to obtain wrinkles by mechanical compression instead of through swelling. Thus, by using different experimental procedures, we could selectively create swelling-induced and mechanically induced wrinkles.

CONCLUSIONS

Serrated structures are formed along the edge of PDMS disks using chemical oxidation by a mixture of sulfuric acid and nitric acid. In the center region of the disk, wrinkles are also formed due to buckling instability, which is induced by the swelling of the oxidized surface layer with the acid solution or water. Because the disk is prepared by vulcanizing a drop of the PDMS prepolymer and the meniscus of the drop is retained after the vulcanization, a thickness gradient is present near the edge of the disk. In addition, the wavelength of the wrinkles depends on the thickness of the underlying PDMS. The combination of this dependency and the thickness gradient resulted in the formation of a serrated structure. This same oxidation method can be used to create small objects with serrated edges. Thus, utilizing the thickness gradient of the sample, various microstructures, which are more complex than a simple stripe pattern, can easily be created.

ACKNOWLEDGMENTS

This work was supported by a grant from the Ministry of Education, Culture, Sports, Science and Technology of Japan (Grant-in-Aid for Scientific Research (C), No. 25410223).

REFERENCES

1. Penkov, B.; Bordonaro, G.; Golovin, A. B.; Bendoym, I.; Tennant, D. M.; Crouse D. T. *J. Micro-Nanolithogr. MEMS MOEMS* **2013**, *12*, 033009.

2. Ariga, K.; Hill, J. P.; Lee, M. V.; Vinu, A.; Charvet, R.; Acharya, S. *Sci. Technol. Adv. Mater.* **2008**, *9*, 014109.
3. Walther, A.; Muller, A. H. E. *Chem. Rev.* **2013**, *113*, 5194.
4. Ward, M. D.; Raithby, P. R. *Chem. Soc. Rev.* **2013**, *42*, 1619.
5. Ariga, K.; Yamauchi, Y.; Rydzek, G.; Ji, Q.; Yonamine, Y.; Wu, K. C.-W.; Hill, J. P. *Chem. Lett.* **2014**, *43*, 36.
6. Ariga, K.; Yamauchi, Y.; Mori, T.; Hill, J. P. *Adv. Mater.* **2013**, *25*, 6477.
7. Ariga, K.; Vinu, A.; Yamauchi, Y.; Ji, Q.; Hill, J. P. *Bull. Chem. Soc. Jpn.* **2012**, *85*, 1.
8. Rodriguez-Abreu, C.; Shrestha, R. G.; Shrestha, L. K.; Harush, E.; Regev, O. *J. Nanosci. Nanotechnol.* **2013**, *13*, 4497.
9. Sorrenti, A.; Illa, O.; Ortuno, R. M. *Chem. Soc. Rev.* **2013**, *42*, 8200.
10. Innocenzi, P.; Malfatti, L. *Chem. Soc. Rev.* **2013**, *42*, 4198.
11. Rao, G. V. R.; Lopez, G. P.; Bravo, J.; Pham, H.; Datye, A. K.; Xu, H.; Ward, T. L. *Adv. Mater.* **2002**, *14*, 1301.
12. Biot, M. A. *Geol. Soc. Am. Bull.* **1961**, *72*, 1595.
13. Bowden, N.; Brittain, S.; Evans, A. G.; Hutchinson J. W.; Whitesides, G. M. *Nature* **1998**, *393*, 146.
14. Watanabe, M. *J. Polym. Sci. Part B: Polym. Phys.* **2005**, *43*, 1532.
15. Kraus, T.; Brodoceanu, D.; Pazos-Perez, N.; Fery, A. *Adv. Funct. Mater.* **2013**, *23*, 4529.
16. Chen, C.-M.; Yang, S. *Polym. Int.* **2012**, *61*, 1041.
17. Ohzono, T.; Monobe, H. *J. Colloid Interface Sci.* **2012**, *368*, 1.
18. Genzer, J.; Groenewold, J. *Soft Matter* **2006**, *2*, 310.
19. Yoo, P. J.; Suh, K. Y.; Park, S. Y.; Lee, H. H. *Adv. Mater.* **2002**, *14*, 1383.
20. Volynskii, A. L.; Bazhenov, S.; Lebedeva, O. V.; Bakeev, N. F. *J. Mater. Sci.* **2000**, *35*, 547.
21. Hyun, D. C.; Moon, G. D.; Park, C. J.; Kim, B. S.; Xia, Y.; Jeong, U. *Adv. Mater.* **2010**, *22*, 2642.
22. Breid D.; Crosby, A. J. *Soft Matter* **2011**, *7*, 4490.
23. Watanabe, M. *Soft Matter* **2012**, *8*, 1563.
24. Shih, T.-K.; Ho, J.-R.; Chen, C.-F.; Whang, W.-T.; Chen, C.-C. *Appl. Surf. Sci.* **2007**, *253*, 9381.
25. Watanabe, M.; Mizukami, K. *Macromolecules* **2012**, *45*, 7128.
26. Lin, P.-C.; Yang, S. *Appl. Phys. Lett.* **2007**, *90*, 241903.
27. Chen, X.; Hutchinson, J. W. *J. Appl. Mech.* **2004**, *71*, 597.
28. Chung, J. Y.; Nolte, A. J.; Stafford, C. M. *Adv. Mater.* **2009**, *21*, 1358.
29. Cai, S.; Breid, D.; Crosby, A. J.; Suo, Z.; Hutchinson, J. W. *J. Mech. Phys. Solids.* **2011**, *59*, 1094.
30. Kawamura, E.; Horiguchi, G.; Tsukaya, H. *Plant J.* **2010**, *62*, 429.
31. Chung, J. Y.; Nolte, A. J.; Stafford, C. M. *Adv. Mater.* **2011**, *23*, 349.
32. de Gennes, P.-G.; Brochard-Wyart, F.; Quere, D. Capillarity and Wetting Phenomena; Springer-Verlag: New York, **2004**; Chapter 4.
33. Yan, Y.; Wang, B.; Yin, J.; Wang, T.; Chen, X. *Appl. Phys. A* **2012**, *107*, 761.
34. Vandeparre, H.; Gabriele, S.; Brau, F.; Gay, C.; Parker, K. K.; Damman, P. *Soft Matter* **2010**, *6*, 5751.